CHAPTER 2

THEORETICAL BACKGROUND

In this chapter, the theoretical aspect that involves the properties of zinc oxide and the sputtering process will be described.

2.1 Properties of Zinc Oxide Thin Films

Recently, ZnO films have attracted more interests as a transparent conductive film. ZnO materials consist of a low cost and abundant materials, which can be readily produced for large–scale coating. They have low growth temperature, non–toxicity and ease of doping with group III elements for higher conductivity.

ZnO is a II–VI compound semiconductor and belongs to the class of direct wide bandgap of wurtzite structure. The unit cell of this structure is shown in Fig. 2.1. The transparency in the visible wavelength region is due to their large energy gap $E_g > 3$ eV. The basic material parameters of ZnO are shown in Table 2.1.

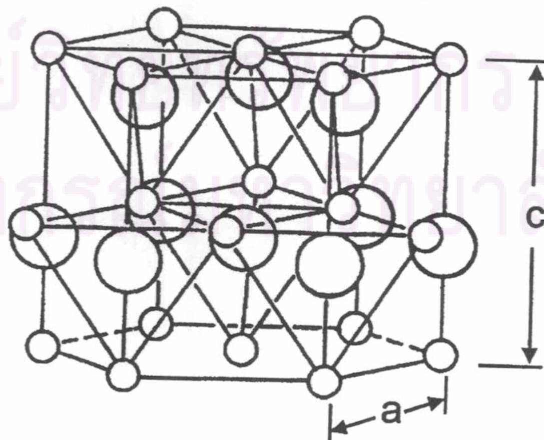

Figure 2.1: Unit cell of ZnO crystal. Small circles are zinc atoms and large circles represent oxygen atoms.

Table 2.1: Properties of wurtzite ZnO [3,4].

Property	Value
Mineral name	zincite
Energy gap (eV)	3.4 (direct)
Melting point (°C)	1975
Melting point of metal (°C)	420
Heat of formation (eV)	3.6
Dissociation energy (eV)	2.9
Density (g/cm^3)	5.67
Crystal structure, space group	hexagonal, wurtzite
Refractive index	2.008, 2.029
Dopants	B, Al, In, Ga, Si, Sn, F, Cl
Lattice parameters at 300 K: (nm)	a: 0.32495, c: 0.52069
Linear expansion coefficient (/ °C)	a: 6.5×10^{-6}, c: 3.0×10^{-6}
Intrinsic carrier concentration	$<10^6$ cm^{-3} (max n–type doping$>10^{20}$ cm^{-3} electrons; max p–type doping $<10^{17}$ cm^{-3} holes

2.2 Intrinsic Donor and Extrinsic Donor

As typical representatives of compound semiconductors shown in Fig. 2.2, conductivity in ZnO can arise from intrinsic (defects) or extrinsic (dopants) charge carriers. If this semiconductor is perfectly prepared without intrinsic or extrinsic dopants (see the dashed–circle in Fig. 2.2), its resistivity is very high (of the order of $> 10^7$ Ω·cm) [3] and the semiconductor becomes an insulator. Furthermore, the transparency in the long wavelengths region (photon energies less than the bandgap) is very high due to low free carrier concentration. Nevertheless the low resistivity can be achieved in two ways:

(1) Creation of intrinsic donors by lattice defects (oxygen vacancies or Zn interstitial atoms).

(2) Introduction of extrinsic dopants of group III elements such as Al, Ga with one addition conduction electron on Zn sites.

The first way can be achieved during the deposition by carefully adjusting the oxygen partial pressure and the deposition rate, or a reduction of the oxide after deposition, by annealing under vacuum. This can cause some oxygen atoms missing from suitable sites in the crystal structure. This kind of defect is called the *oxygen vacancy*. Furthermore some Zn atoms may be located between the lattice sites. This type of defect is called the *zinc (Zn) interstitial atom*. Both defects are referred as the *intrinsic donors*. Electrons generated from the oxygen vacancies and the Zn interstitial atoms primarily dominate the conduction characteristics of ZnO. The attained resistivity is typically in the order of > 10^{1} Ω·cm [18–20]. However, it has been found that such films exhibit properties which are not well suitable for applications. They are not stable under ambient conditions especially at higher temperatures due to the re–oxidation of the oxygen–deficient films or re–organization of ZnO structures.

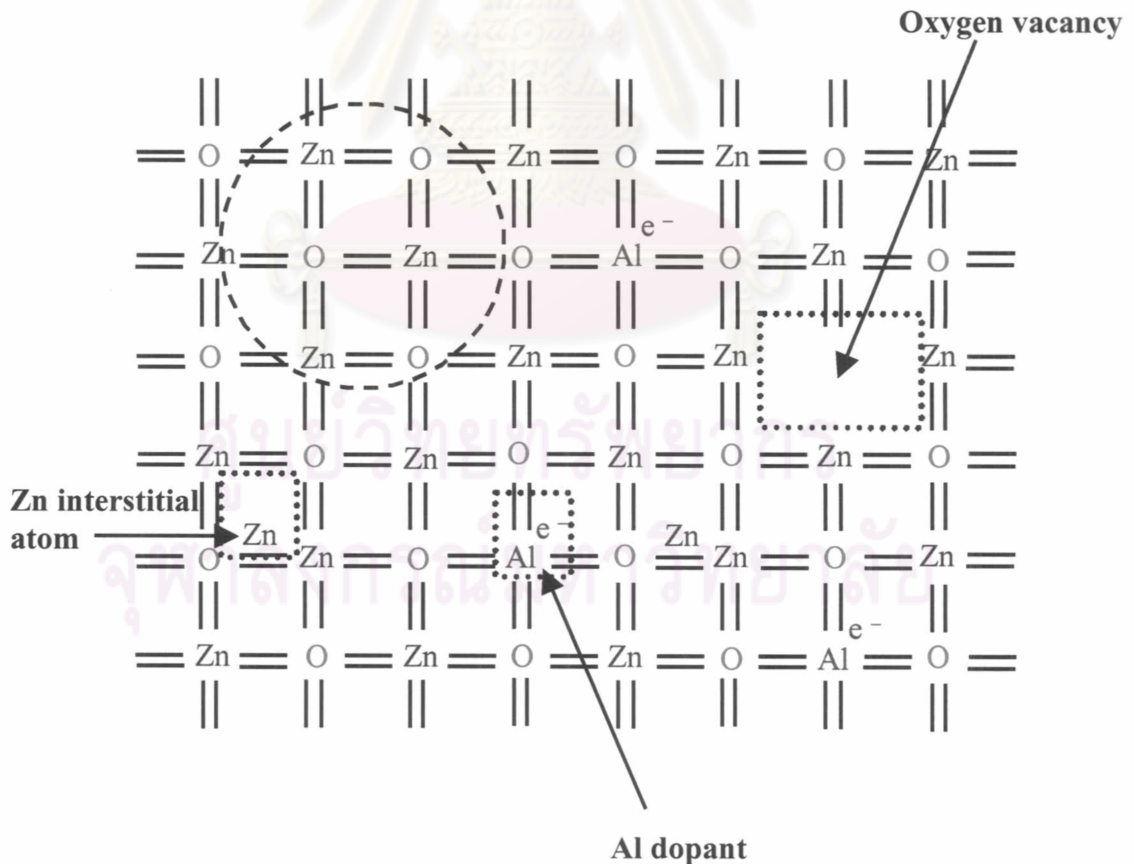

Figure 2.2: Structure of ZnO compound showing intrinsic defects and extrinsic dopants.

For the second way, these dopants are called *extrinsic donors*. The attained resistivity is in the order of < 10^{-3} Ω·cm [21–24]. The electrical conductivity of the Al–doped ZnO films is higher than that of the pure ZnO films, due to the contribution from Al ions on substitution sites of Zn ions, as well as from oxygen vacancies and Zn interstitial atoms but transparency near infrared may be lost due to increasing of free carrier concentration.

2.3 Preparation Method of ZnO Thin Films

ZnO thin films can be prepared by various methods such as chemical vapour deposition, pulsed laser deposition, spray pyrolysis and magnetron sputtering. Among these methods, the magnetron sputtering is preferential by several advantages [3]: (1) low substrate temperature (down to room temperature); (2) good adhesion of films on substrates; (3) very good thickness uniformity over relatively large area and high density of the films; (4) directive deposition from elemental (metallic) targets by reactive sputtering in reactive gas mixtures, and (5) scalability to large areas. Therefore the magnetron sputtering is the most widely used technique for preparing ZnO or ZnO(Al) films. For deposition of pure ZnO films, a Zn target is used in argon and oxygen gas ambient, but for ZnO(Al) films, two types of targets are applicable according to the Al doping method. One is the co–sputtering of an Al metallic target and a pure ZnO ceramic target, the other is the conventional sputtering of a $ZnO+Al_2O_3$ ceramic target. There have been numerous reports concerning the influence of argon gas pressure, sputtering power, substrate temperature, oxygen partial pressure on the ZnO(Al) films quality. The results from the literatures for magnetron sputtered ZnO and doped ZnO films are summarized in Table 2.2.

Table 2.2: Compilation of electrical parameters of ZnO films prepared by magnetron sputtering.

Films	Reference (year)	Target	T_{sub} (°C)	*P* (Pa)	Method[a]	ρ (Ω·cm)	*n* (cm^{-3})	μ (cm^2/Vs)
ZnO	Gao *et al* [18] (2004)	ZnO	–[b]	0.66	DCMS	3.7×10^{5}	–	–
				1.33	DCMS	10^{6}	–	–
ZnO	Ondo-Ndong *et al* [19] (2003)	Zn	100	0.4	RFRMS	10^{12}	–	–
ZnO	Uthanna *et al* [20] (2002)	Zn	300	0.6	RFRMS	4.0×10^{1}	–	–
ZnO(Al)	Song *et al* [14] (2002)	ZnO: Al_2O_3 2 wt%	250	0.2	RFMS	2.7×10^{-4}	–	–
ZnO(Al)	Igasaki *et al* [21] (2002)	ZnO: Al_2O_3 2 wt%	100	0.13	RFMS	2.5×10^{-4}	8.0×10^{20}	20
ZnO(Sc)	Minami *et al* [25] (2000)	ZnO: Sc_2O_3 2 wt%	200	0.8	DCMS	3.1×10^{-4}	6.9×10^{20}	29
ZnO(Al)	Ellmer *et al* [22] (1998)	ZnO: Al	–[b]	0.8	RFMS	5.7×10^{-4}	3.5×10^{20}	31
ZnO(Al)	Jäger *et al* [23] (1998)	Zn: Al	300	0.21	DCRMS	4.2×10^{-4}	2.6×10^{20}	57
		Zn: Al	300	0.15	ACRMS	4.0×10^{-4}	4.9×10^{20}	32
ZnO(Al)	Park *et al* [13] (1998)	ZnO: Al_2O_3 3 wt%	150	0.2	RFMS	4.7×10^{-4}	7.5×10^{20}	15
ZnO(Al)	Martinez *et al* [24] (1997)	Zn: Al 2 at%	380	–	RFRMS	6.0×10^{-4}	4.0×10^{20}	29
		ZnO: Al 2 at%	200	–	RFMS	1.0×10^{-3}	3.0×10^{20}	11
		ZnO: Al_2O_3 2 wt%	200	–	RFMS	6.0×10^{-4}	3.0×10^{20}	17
		ZnO: Al_2O_3 2 wt%	25	–	RFMS	3.5×10^{-3}	4.0×10^{19}	7

[a]DCRMS is DC reactive magnetron sputtering, RFRMS is RF reactive magnetron sputtering, ACRMS is AC reactive magnetron sputtering, RFMS is RF magnetron sputtering, and DCMS is DC magnetron sputtering.

[b]No external heating.

ศูนย์วิทยทรัพยากร
จุฬาลงกรณ์มหาวิทยาลัย

2.4 Principles of Sputtering

Sputtering is a physical phenomenon involving the acceleration of ions, usually Ar^+, through electric field and the bombardment by these ions on a target or cathode. The momentum is transferred from ions to atoms of target, possibly leading to the ejection of one of these atoms. This process is known as *sputtering*. After sputtering, the atoms can move through space until they strike and condense on the surface of a receiver, which is known as a *substrate*. By repeating the process over and over, coating of many atomic or molecular layers of target material on the substrate can build up. The coating, which is generally less than 1 μm thick, is called a *thin film* and the process is known as *sputtering deposition*.

2.4.1 Ion–Surface Interactions

Let us consider what happens when an ion knock on the surface of the target. One or all of the following phenomena may occur (Fig. 2.3):

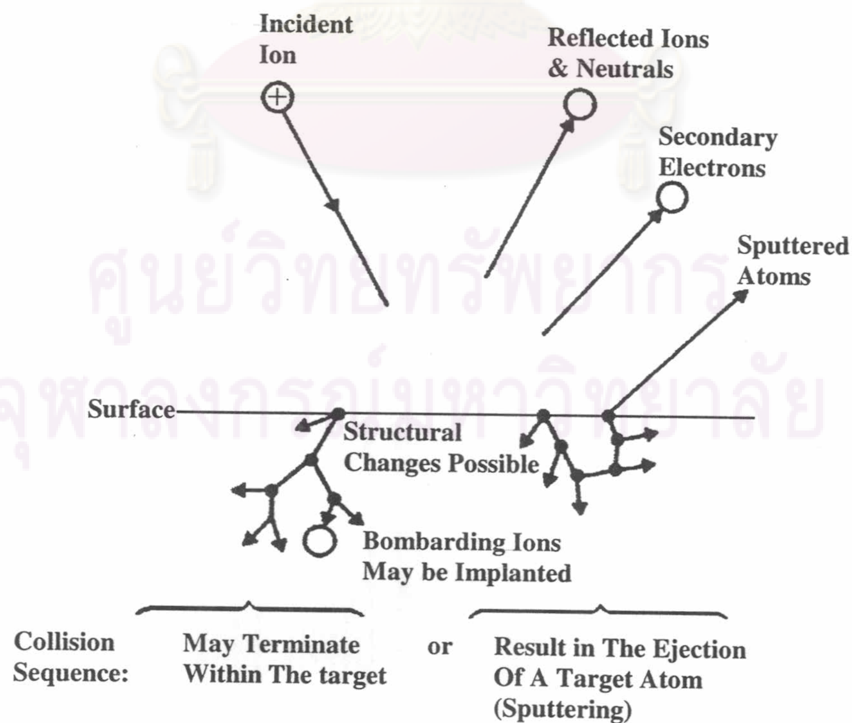

Figure 2.3: Interactions of ions with surface [26].

(1) The ion may be reflected, probably being neutralized in the process.

(2) The impact of the ion may cause the target to eject an electron, referred to as a secondary electron.

(3) The ion may become buried in the target. This is the phenomenon of ion implantation.

(4) The ion impact may also be responsible for some structural rearrangement in the target material.

(5) The ion impact may set up a series of collision between atoms of the target, possibly leading to the ejection of one of these atoms, the process is known as sputtering.

2.4.2 Mechanism of Sputtering

The sputtering process can sometime simply be compared to a model of atomic billiard as shown in Fig. 2.4. The cue ball (the bombarding ion) strikes the arranged pack of ball (the atomic array of the target) resulting in the scattering of the balls (target atoms) in all directions, including some back towards the player (out of the target surface). The model resembles the sputtering process. The billiard model is not too unrealistic, however the interatomic energy is still neglected. Nevertheless, it can somewhat explain the sputtering process better than the other models.

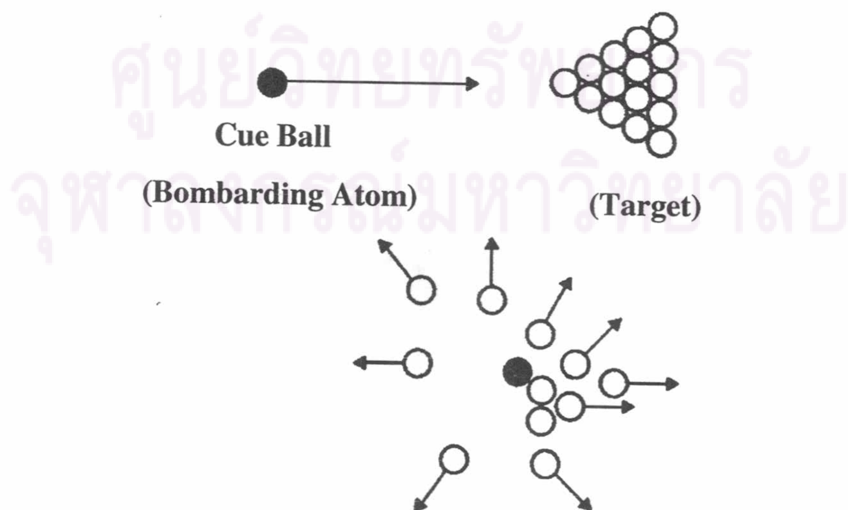

Figure 2.4: Sputtering–the atomic billiards game [26].

ศูนย์วิทยทรัพยากร
จุฬาลงกรณ์มหาวิทยาลัย

2.4.3 Glow Discharges and Plasma

Considering the simplified sputtering system shown in Fig. 2.5 (a). The target is a plate of materials to be deposited. It is connected to the negative terminal of a DC or RF power supply, and is known as the *cathode*. The high voltage is applied to the cathode. The substrate that faces the cathode may be ground, electrically floating, biased positively or negatively, heated, cooled, or some combination of these and generally called the *anode*. After evacuation of the chamber, a sputtering gas, typically argon gas is introduced as the medium in which a discharge is initiated and sustained.

When the voltage V is applied between the electrodes, the electric field ($E = V/d$) is generated, where d is cathode–to–anode distance. A very small current flows at first due to a small number of initial charge carriers in system. The initial charge carriers (primary electrons) are generated by cosmic ray. As the voltage is increased, sufficient energy is imparted to the charge particles to create more carriers. This occurs through ion collision ionization of neutral gas atoms.

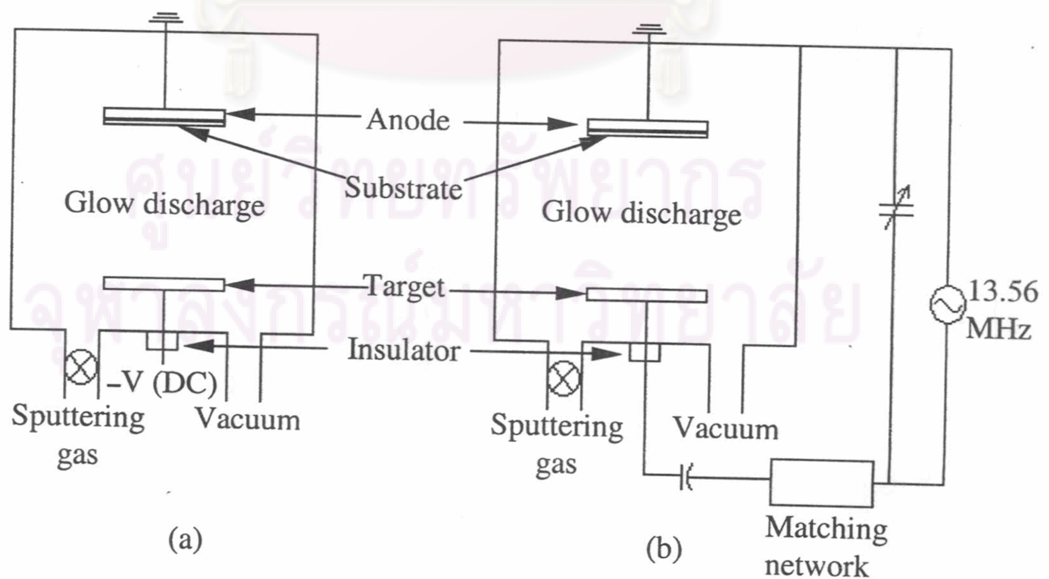

Figure 2.5: Schematics of simplified sputtering: (a) DC, (b) RF [27].

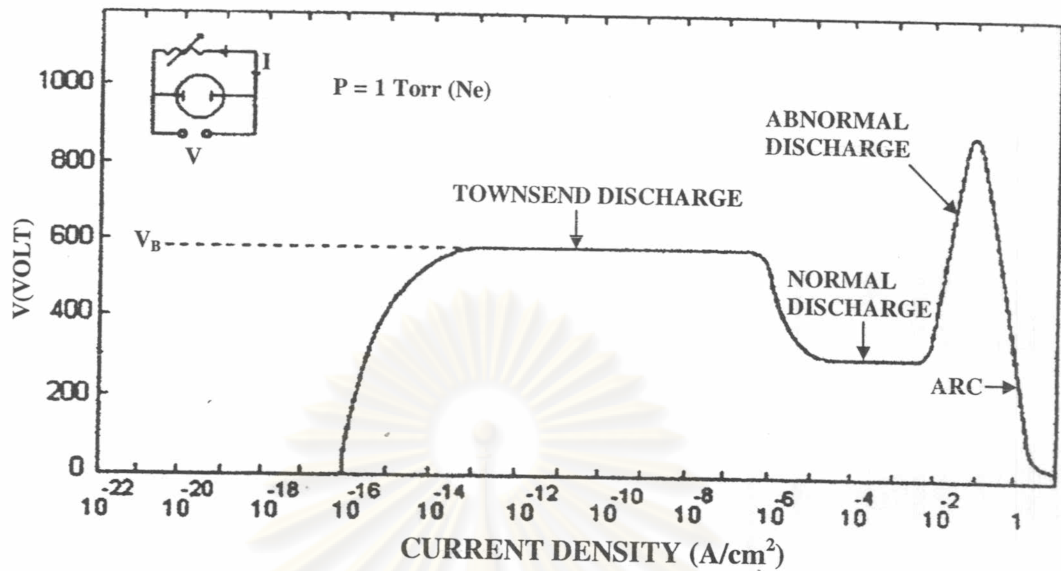

Figure 2.6: The voltage of electrodes vs. current density of DC glow discharge [17].

With charge multiplication, the current increases rapidly, but the voltage, limited by the output of the power supply, remains constant. This is known as the *Townsend discharge* and the constant voltage is called *breakdown voltage* (V_B) as shown in Fig. 2.6.

Large number of electrons and ions are created through avalanches. Ultimately, with enough number of electrons, the discharge becomes self–sustaining. The gas begins to glow, the voltage drops, accompanied by increasing in current. This stage is a *normal discharge*. As more power is applied, the bombardment increasingly spreads over the entire surface until a nearly uniform current density is achieved. A further increase in the power results in higher voltage and current density. The *abnormal discharge* regime has now been entered, and this is the operative domain for sputtering process.

2.4.4 Collision Processes

Collisions between electrons and all other species (charged or neutral) within the plasma dominate the properties of the glow discharge. The collisions can be either elastic or inelastic, depending on whether the internal energy of the colliding species

is preserved. In the elastic collision, only kinetic energy is interchanged, no atomic excitation occurs and the potential energy is conserved. The well–known result for elastic binary collisions is [27]

$$\frac{E_2}{E_1} = \frac{4M_1M_2}{(M_1+M_2)^2}\cos^2\theta, \tag{2.1}$$

where 1 and 2 refer to the two particles of mass M_i and energy E_i ($i = 1,2$). Here we assume that M_2 is initially stationary and M_1 collides with it at an angle θ defined by the initial trajectory and the line joining their centers at contact. The quantity $4M_1M_2/(M_1+M_2)^2$ is known as the *energy transfer function*. For example, the collision between a moving electron and a stationary gas molecule ($M_1 \ll M_2$), the energy transfer function is approximately $4M_1/M_2$. That is, small kinetic energy is transferred in the collision of the light electron with the massive gas atom.

Now, consider inelastic collisions. The change in internal energy (ΔU) of the struck particle must now be accounted for in the condition requiring conservation of energy. The maximum fraction of kinetic energy transferred is given by [27]

$$\frac{\Delta U}{(1/2)M_1v_1^2} = \frac{M_2}{M_1+M_2}\cos^2\theta, \tag{2.2}$$

where v_1 is the initial velocity of particle 1. For the inelastic collision between an electron and a gas molecule when $\cos\theta = 1$, $\Delta U/(1/2)M_1v_1^2 \approx 1$, which mean that all of an electron's kinetic energy can be transferred to the heavier species in the inelastic collision.

ศูนย์วิทยทรัพยากร
จุฬาลงกรณ์มหาวิทยาลัย

The diversity of inelastic collision and chemical processes that occur in plasmas are summarized as the followings [27]:

(1) Ionization. The most important process in sustaining the discharge is electron impact ionization. In this process, a bound electron in an atom is ejected. A typical reaction is

$$e^- + Ar \rightarrow Ar^+ + 2e^-. \tag{2.3}$$

By this multiplication mechanism the glow discharge is sustained. The reverse reaction is known as a recombination; an electron combines with a positive ion to form a neutral atom.

(2) Excitation. In this process, the energy transferred to the bound electron is less as compared with that of the ionization process. It enables the electron to jump only to a higher energy level. This process is known as excitation. An example is

$$e^- + Ar \rightarrow Ar^* + e^-. \quad (2.4)$$

(3) Dissociation. In dissociation, the molecule is broken into smaller atomic or molecular fragments such as dissociation of CF_4, i.e.

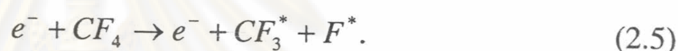

$$e^- + CF_4 \rightarrow e^- + CF_3^* + F^*. \quad (2.5)$$

(4) Dissociative ionization. During dissociation one of the excited species may become ionized, e.g.

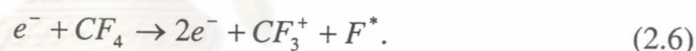

$$e^- + CF_4 \rightarrow 2e^- + CF_3^+ + F^*. \quad (2.6)$$

(5) Electron attachment. In this case, neutral molecule becomes negative ions after capturing an electron. For example,

$$e^- + SF_b^0 \rightarrow SF_b^-. \quad (2.7)$$

(6) Dissociative attachment.

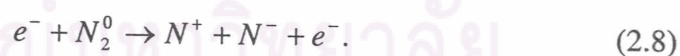

$$e^- + N_2^0 \rightarrow N^+ + N^- + e^-. \quad (2.8)$$

(7) Symmetrical charge transfer. The probability of collision leading to exchange of charge, e.g.

$$A + A^+ \rightarrow A^+ + A. \quad (2.9)$$

ศูนย์วิทยทรัพยากร
จุฬาลงกรณ์มหาวิทยาลัย

(8) Asymmetric charge transfer. Similar to process (7), the probability of collision leading to exchange of charge between unlike system, e.g.

$$A + B^{+} \rightarrow A^{+} + B. \tag{2.10}$$

(9) Metastable–Neutral. When a metastable atom collides with a neutral, the neutral can become ionized if its ionization energy is less than the excitation energy of the excited atom:

$$A^{*} + B \rightarrow B^{+} + A + e^{-}. \tag{2.11}$$

(10) Metastable–Metastable ionization.

$$A^{*} + A^{*} \rightarrow A + A^{+} + e^{-}. \tag{2.12}$$

The processes (1) and (2) can be used to explain the overview of the grow discharge and the other processes (processes (3) to (10)) are observed in reactive sputtering, plasma etching system, which were not being interested in this work.

2.5 RF Magnetron Sputtering

RF sputtering was invented as a mean of depositing insulating thin films. This technique uses an alternating voltage power supply at RF frequencies ranging from 5 to 30 MHz. However, 13.56 MHz has been reserved for processing by the Federal Communications Commission (FCC) and is widely used [27]. The basic feature of a magnetron discharge is the confinement of the plasma in front of the target (cathode). This is achieved by a combination of electric and magnetic fields. The magnetic field strength is adjusted in such a way (about 50 to 200 mT) that the electrons are significantly influenced by the magnetic field while the ions are not. The electrons perform cycloidal orbits in the crossed electric and magnetic fields, leading to very high ionization efficiency.

2.5.1 Electron Motion in Parallel Electric and Magnetic Fields

When a magnetic field of strength $\vec{B}$ is superimposed on the electric field $\vec{E}$ between the target and substrate, electrons within the dual fields environment experiences the magnetic force in addition to electric force, i.e. (Lorentz force)

$$\vec{F} = \frac{mdv}{dt} = -q(\vec{E} + \vec{v} \times \vec{B}), \tag{2.13}$$

where $q, m,$ and v are the charge, mass, and velocity of the electron, respectively.

Consider the case where $\vec{B}$ and $\vec{E}$ are parallel as shown in Fig. 2.7 (a). When the electrons are emitted exactly normal to the target surface and parallel to both fields, only the electric field accelerates them toward the anode. Next consider the case where the $\vec{E}$ field is neglected but $\vec{B}$ is still applied as shown in Fig 2.7 (b). If the electron is launched from the cathode with a velocity v at an angle θ with respect to $\vec{B}$, it experiences a force $qvB\sin\theta$ in the direction perpendicular to $\vec{B}$. The electron orbits in a circular motion with a radius $r = mv\sin\theta / qB$. The electron motion is helical and spiral with constant velocity $v\cos\theta$.

For the case where $\vec{B}$ and $\vec{E}$ are parallel as shown in Fig 2.7 (c), when the electrons are launched at an angle θ, corkscrew motion with constant radius occurs, but because of electron acceleration in the $\vec{E}$ field, the pitch of the helix lengthens with time. With the time varying $\vec{E}$ fields, it complicates the situation further and electron spirals of variable radius can occur. Clearly, magnetic fields prolong the electron residence time in the plasma and thus enhance the probability of ion collisions. This leads to larger discharge currents and increases sputter deposition rates.

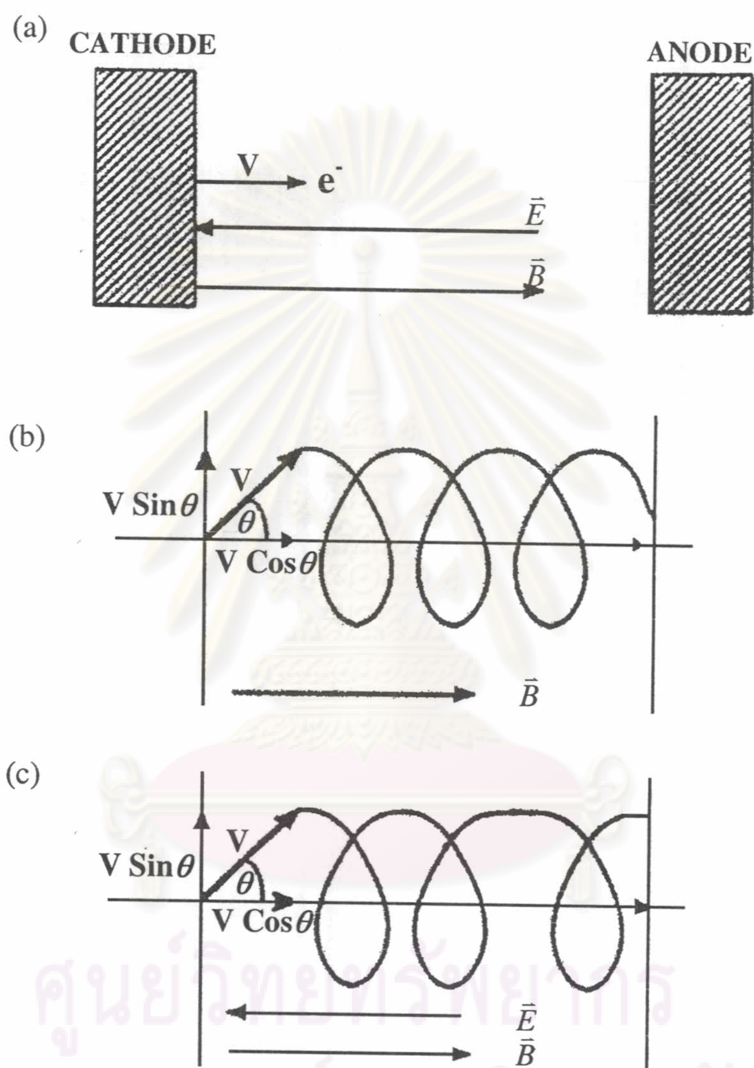

Figure 2.7: The effect of $\vec{E}$ and $\vec{B}$ on electron motion. (a) Linear electron trajectory when $\vec{E} // \vec{B}$ ($\theta = 0$); (b) Helical orbit of constant pitch when $\vec{B} \neq 0, \vec{E} = 0, (\theta \neq 0)$; (c) Helical orbit of variable pitch when $\vec{E} // \vec{B}$ ($\theta \neq 0$) [27].

ศูนย์วิทยทรัพยากร
จุฬาลงกรณ์มหาวิทยาลัย

2.5.2 Electron Motion in Perpendicular Electric and Magnetic Fields

In magnetron, electrons ideally do not even reach the anode but are confined near the target surface, increasing the ionizing efficiency there. This is accomplished by employing a magnetic field oriented parallel to the target and perpendicular to the electric field as shown schematically in Fig. 2.8. This is achieved by placing a ring, a bar and a horseshoe magnet behind the target. The electrons emitted from the cathode are initially accelerated toward the anode, executing a helical motion, but they are bent in an orbit back to the target surface in very much the same way. By suitable orientation of target magnets, target erosion by sputtering occurs within this track because ionization of the working gas is most intense above it.

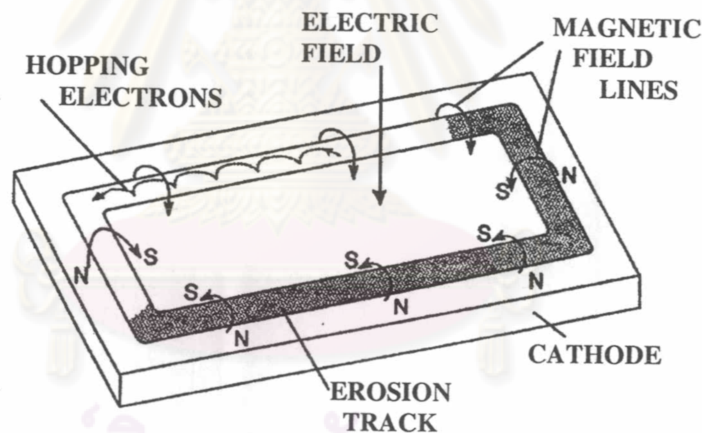

Figure 2.8: Applied fields and electron motion in the plasma magnetron [27].

2.6 Thin Film Formation [26]

In the sputtering deposition, materials arrive at the substrate are mostly in the form of atoms or molecules (Fig. 2.9). The deposited atom diffuses around the substrate with a motion determined by its binding energy to the substrate and is influenced by the temperature of the substrate. The atom will either evaporate from the surface or join

with another diffusing single atom to form a doublet, which is less mobile but more stable than the single atom.

(a) Single Atom Arrives

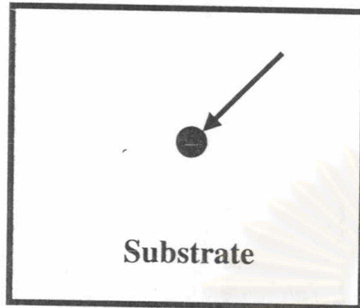

(e) Growth

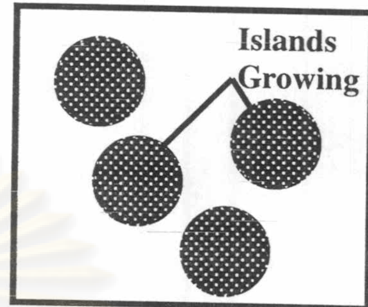

(b) Migration Re–evaporation

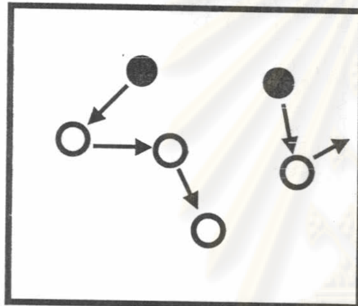

(f) Island Shape

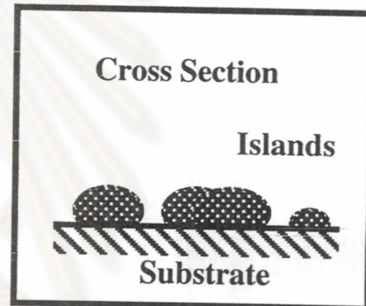

(c) Collision & Combination of Single Atoms

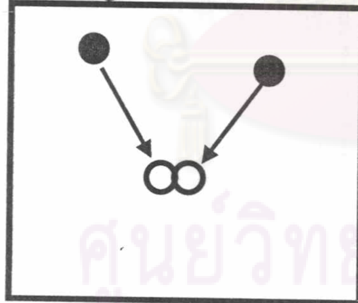

(g) Coalescence

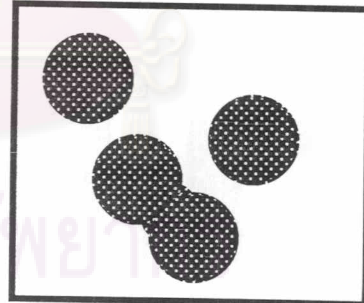

(a) Nucleation

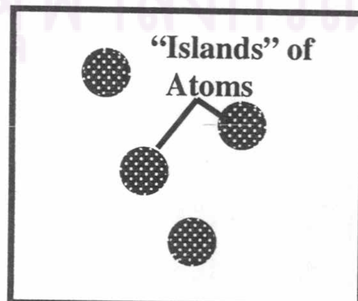

(h) Continuity

Figure 2.9: Formation of thin films [26].

The opportunity of forming the atomic pair depends on the single atom density and hence on the arrival or deposition rate. In time, the doublets will be joined by other single atoms to form triplets, quadruplet and so on. This is the *nucleation stage* of thin film growth, leading to the formation of quasi–stable *islands*, each containing tens or hundreds of atoms. During the *island growth* stage, the islands grow in size rather than in number. When they grow large enough to connect to each other, this stage is known as the *coalescence stage*. The coalescence proceeds until the film reach *uniformity*, but this may not occur in some cases until the film is several hundred Å in average thickness.

During the island stage, each island is usually single crystal or contains just a few crystals. On a polycrystalline substrate, the orientation of each island will be random. On a single crystal substrate, the island orientations may be determined by the substrate structure so that growth leads to a single crystal film. This is the phenomenon of *epitaxy growth*.

If the surface atoms are mobile, they have a greater opportunity of finding low energy position, consistent with crystal growth, in the growing film. But since it also takes time to find an energetically favorable lattice position, therefore the crystal growth is also encouraged by low deposition rate. Nevertheless, we can enhance the formation time of atoms by increasing the substrate temperature, in which the mobility of atoms is enhanced. So the high substrate temperature and low deposition rate lead to large and uniform film thickness. All of the relationships above, the structural of the growing film was found to be extremely sensitive to deposition conditions.

ศูนย์วิทยทรัพยากร
จุฬาลงกรณ์มหาวิทยาลัย